

Experimental evidence for a mechanical function of the cellulose microfibril angle in wood cell walls

A. REITERER[†], H. LICHTENEGGER[‡], S. TSCHEGG[‡] and P. FRATZL[§]

[†] Institut für Meteorologie und Physik, Universität für Bodenkultur, Türkenschanzstraße 18, A-1180 Wien, Austria

[‡] Institut für Materialphysik, Universität Wien, Strudlhofgasse 4, A-1090 Wien, Austria

[§] Erich Schmid Institut der Österreichischen Akademie der Wissenschaften und Montanuniversität Leoben, Jahnstraße 12, A-8700 Leoben, Austria

[Received 17 August 1998 and accepted in revised form 29 October 1998]

ABSTRACT

Wood is a natural fibre composite with a hierarchical cellular structure of a specific strength and a specific modulus of elasticity that can be compared with those of other common construction materials. Each wood cell is typically built of cellulose fibrils spiralling around the macroscopic fibre direction. While it is natural to assume a relation between the microfibril angle (MFA) and the mechanical properties, a good correlation has up to now only been established for single fibres, where a larger extensibility was found for fibres with larger MFA. In the present paper, we show for the first time that this relation even exists for thin (200 μm) sections of wood, which provides strong evidence for the fact that the MFA optimizes the extensibility of wood. In a combination of tensile tests with structural investigations by small angle X-ray scattering on the same sample of *Picea abies*, we found a remarkable increase in maximum strain with increasing MFA, and also a change in the elastic moduli.

§ 1. INTRODUCTION

The mechanical properties of wood can be best understood by reference to its structure. Softwoods like *Picea abies* are appropriate for investigating this relationship as they show a relatively simple cellular structure. According to current cell wall models (Fengel and Wegener 1989) *Picea abies* consists to 95% of tracheids, hollow tubes, oriented approximately in the same direction as the trunk or branch. Their average diameter is 20 μm and their average length is about 3 mm. The cell wall is built up by several layers, the thickest layer being called S2. In spruce tracheids, S2 represents 80–86% of the cell wall (Fengel and Wegener 1989). It consists of partially crystalline elementary cellulose fibrils embedded in an amorphous hemicellulose–lignin matrix. The elementary fibrils are aligned parallel to each other and wind round the cell wall at an angle which is usually called the microfibril angle (MFA). The diameter of a single elementary fibril had been found to be 2.5 nm (Jakob *et al.* 1995). As the S2 represents the major component of the cell wall, the structure of the S2 plays a key role in determining the mechanical properties of the wood cell. It had been reported that the MFA has a certain influence on the stiffness

|| Email: fratzl@unileoben.ac.at.

(Cave 1969, Cave and Walker 1984) and the shrinkage (Meylan 1968) of *Pinus radiata*. A good correlation between the mechanical properties and the MFA had been established for single fibres (Page *et al.* 1971, Page and El-Hosseiny 1983). In the present paper we compare the results from tensile tests on earlywood and latewood samples of a single stem and on samples from the lower and upper side of a branch of *Picea abies* with the results of structural investigations by small angle X-ray scattering on the same samples. Our goal was to investigate the relationship between the MFA and the mechanical properties.

§ 2. EXPERIMENTAL METHODS

2.1. Tensile test on microtome sections

In order to investigate the mechanical characteristics of the wood cell wall we cut 200 μm thick slices in tangential planes exclusively from the earlywood and latewood region throughout 27 annual rings of a single stem (from the 17th–44th annual rings) and from two annual rings in the top (10th and 11th ring) and bottom (18th and 19th ring) of a branch by using a sledge microtome. The ends of the samples were pasted to a 1 mm thick foil (figure 1 (a)) to prevent damage of the samples when gripped in the jaws of a standard testing machine. The tensile measurements were carried out at a constant crosshead speed of 0.2 mm min^{-1} . The moisture content of the sample was kept above the fibre saturation point, where moisture content does not influence the structure and the mechanical properties remain constant (see, for example, Dinwoodie (1989)).

From the tensile tests, stress–strain curves were evaluated. The linear region of these curves was used to determine the modulus of elasticity (figure 1 (b)). This experimental modulus of elasticity is heavily influenced by density. Usually the

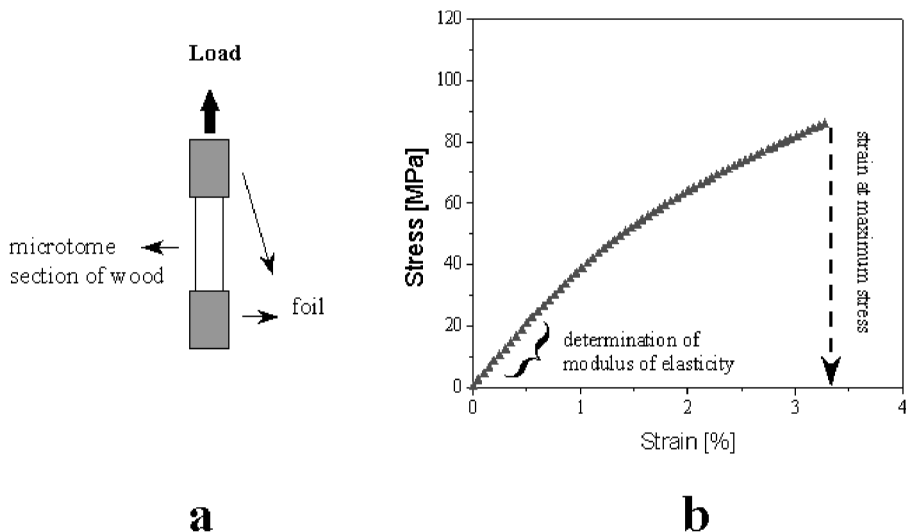


Figure 1. (a) Microtome section of wood used in tensile test and (b) evaluation of modulus of elasticity and strain at maximum stress from stress–strain curves.

density of latewood of *Picea abies* is between two and three times higher than the density of earlywood (Fengel and Wegener 1989). We measured the density of each sample and normalized the modulus of elasticity, E , by the ratio of the calculated density of the cell wall material, ρ_0 , to the experimental density of the sample, ρ , to obtain values

$$E^* = E \rho_0 / \rho, \quad (1)$$

which are independent of density. The density of the cell wall material, ρ_0 , was calculated using average values for the percentages (40% cellulose, 32% hemicellulose and 28% lignin in the stem and the top of the branch under tension; 30% cellulose, 32% hemicellulose and 38% lignin for the wood of the bottom of the branch under compression (Fengel and Wegener 1989)) and the densities ($\rho_{\text{Cellulose}} = 1550 \text{ kg m}^{-3}$, $\rho_{\text{Hemicellulose}} = 1490 \text{ kg m}^{-3}$, $\rho_{\text{Lignin}} = 1400 \text{ kg m}^{-3}$ (Mark 1967)) of the cell wall constituents. In order to characterize the extensibility, the strain at maximum stress ε_{max} was evaluated (figure 1 (b)).

2.2. Small angle X-ray scattering on wood

In order to obtain a reliable correlation between mechanical properties of the samples and their structure, the remaining parts of the samples ruptured in the tensile tests were also used for structure investigations by small angle X-ray scattering (SAXS). Without any further sample preparation, they were encapsulated in plastic foils in order to prevent drying and shrinking of the wood cells in the vacuum chamber of the X-ray equipment. The samples were exposed to Cu $K\alpha$ radiation whose wavelength $\lambda = 0.154 \text{ nm}$. SAXS patterns were obtained by a two-dimensional position sensitive detector positioned in a straight line with the source and the sample at a distance of 100 cm from the sample. The scattering intensity $I(\mathbf{q})$ was recorded as a function of the scattering vector \mathbf{q} with modulus $q = |\mathbf{q}| = (4\pi/\lambda) \sin(\theta)$, where 2θ is the angle between the incoming and the scattered X-ray beam. Scattering patterns were recorded with a typical time of half an hour per spectrum to provide sufficient counting statistics. The scattering intensity $I(\mathbf{q})$ was corrected for the background scattering from the encapsulating foil. The experimental set-up consisted of a 12 kW rotating anode X-ray generator used in a point-focus geometry. The incoming X-ray beam had a circular cross-section of 0.6 mm in diameter.

SAXS is generally appropriate for the investigation of objects in the nanometre range, provided that there is sufficient electron-density contrast between the objects under investigation and the surrounding material. With regard to the theory details can be found for instance in Feigin and Svergun (1987), Glatter and Kratky (1982) or Guinier and Fournet (1955). Assuming a two phase system of objects A in a surrounding matrix B, the SAXS intensity can generally be written as

$$I(\mathbf{q}) = I_0 (\rho_A^e - \rho_B^e)^2 \left| \int_V \exp(i\mathbf{q}\mathbf{r}) d^3r \right|^2, \quad (2)$$

where $(\rho_A^e - \rho_B^e)$ is the electron density contrast between the objects under investigation denoted by A and the surrounding material denoted by B. The scattering vector \mathbf{q} may be expressed in polar coordinates (q, χ) , where q is the length of \mathbf{q} and χ is the angle denoting the direction of \mathbf{q} in the detector plane. In wood there is sufficient electron density contrast between the cellulose fibrils and the surrounding hemicellulose-lignin matrix. If one assumes the shape of the cellulose fibrils as being thin

cylinders, the small-angle scattering is given by a disc perpendicular to the longitudinal fibril axis producing a narrow streak on the detector. The orientation of the streak denoted by χ depends on the angle versus the tracheid axis μ and the rotation α of the cellulose fibril around the tracheid axis (figure 2). The plane of observation ($\alpha = 0^\circ$) is perpendicular to the incoming X-ray beam.

The cellulose MFA μ can be extracted from the angular distribution of the scattered intensity if the geometry of the wood cells is considered (Reiterer *et al.* 1998). In the case of cells with rectangular cross-section there is a superposition of four streaks at angles χ given by

$$\tan \chi = -\tan \mu \cos \alpha, \quad (3)$$

where $\alpha = \omega + n\pi/2$ ($n = 0, 1, 2, 3$) corresponding to the four sides of the rectangle. ω is the rotation angle of the sample around the tracheid axis, which is equal to 0 when the square is positioned at right angles to the incoming beam. For $\omega = 0$ two streaks coincide at $\chi = 0$, and two streaks appear at $\chi = \pm\mu$. Hence, at this sample position, μ can be determined directly (Reiterer *et al.* 1998, Lichtenegger *et al.* 1998). In reality it should be assumed that there is not only a single MFA μ , but a distribution of MFAs $g(\mu)$. This leads to a broadening of the streaks, the width of the streak in χ being equal to the width of $g(\mu)$ when $\omega = 0$.

In the case of cells with circular cross-section (for example compression wood at the bottom of the branch) and an unique angle μ , the intensity distribution is proportional to

$$R(\chi) = (\sin^2 \mu - \sin^2 \chi)^{-1}. \quad (4)$$

This distribution peaks at $\chi = \pm\mu$ and is independent of the rotation ω of the sample (see, for example, Preston (1946)). For a distribution of MFAs the situation is more complicated; details can be found, for example, in Perret and Ruland (1969) or Lichtenegger *et al.* (1998).

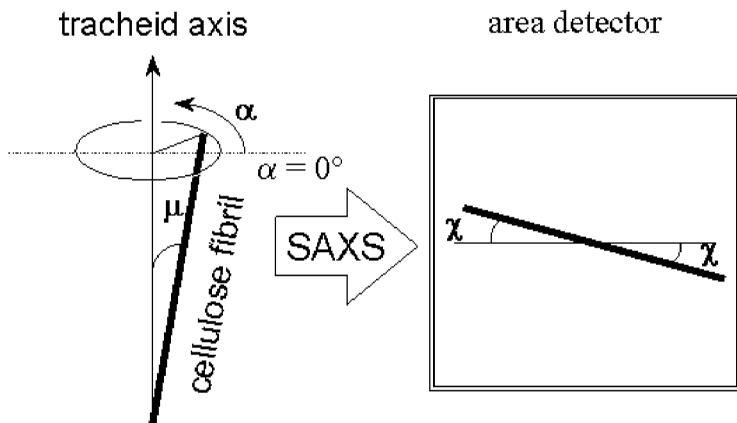


Figure 2. An elementary cellulose fibril tilted by an angle μ with respect to the tracheid axis produces a streak on the area detector. The orientation of the streak depends on μ and the rotation α around the tracheid axis.

§ 3. RESULTS

3.1. Results of the mechanical investigations

In figure 3(a) the results for the normalized modulus of elasticity E^* are shown versus the investigated 27 annual rings of the stem. These density-corrected values for earlywood and latewood were close together but two separate regions could be distinguished. In the first region between the annual rings 17 and 37 the moduli of elasticity E^* of earlywood were higher than those of latewood; in the second region between the annual rings 38 and 44 the E^* values of latewood rose above those of earlywood. Figure 3(b) shows the moduli of elasticity of the annual rings of the

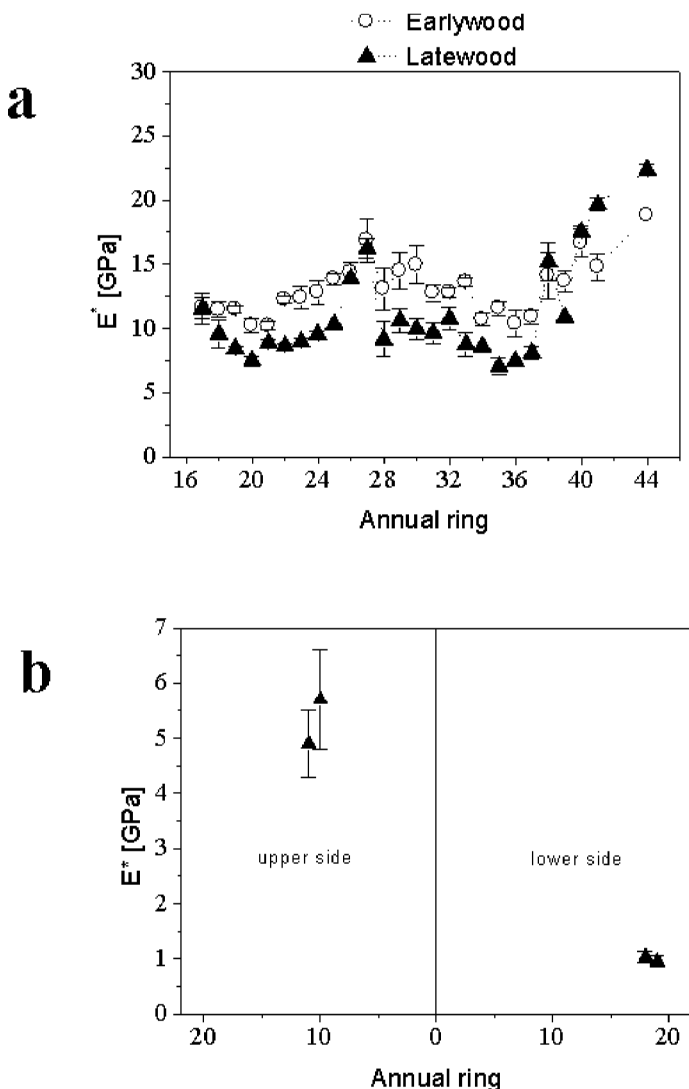


Figure 3. Normalized modulus of elasticity E^* versus the investigated annual rings (a) of the stem and (b) of the branch.

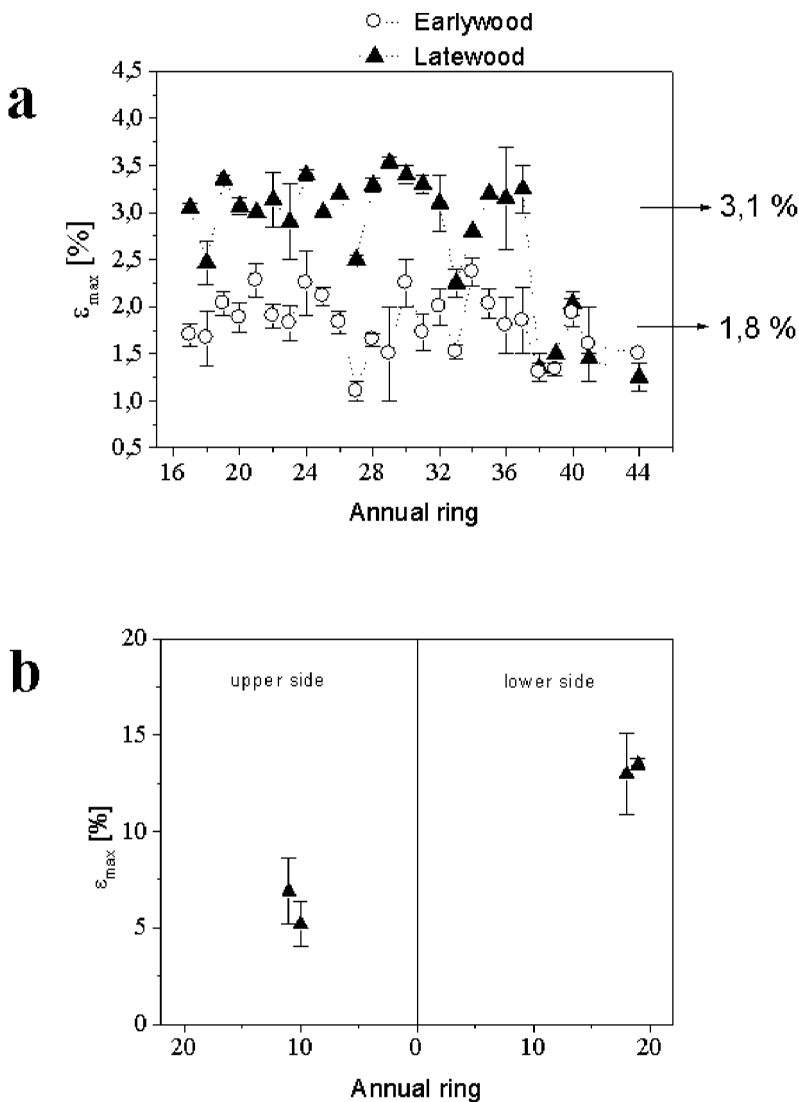


Figure 4. (a) Strain at maximum stress ϵ_{\max} versus the investigated annual rings of the stem. After the annual ring 37 the strain at maximum stress of latewood dropped dramatically. (b) The values for ϵ_{\max} of the branch are much higher than those of the stem.

lower and upper side of the branch. These values were much lower than those of the stem, especially for the lower side, where compression wood had been formed.

The results for the strain at maximum stress ϵ_{\max} of the stem are shown in figure 4(a). This parameter is independent of density and determines the extensibility of the cell walls. Considerable differences in extensibility between earlywood and latewood were found in most annual rings (first region between annual ring 17 and 37). The earlywood of these annual rings could be stretched by $\approx 1.8\%$ and latewood by $\approx 3.1\%$ prior to macrocrack initiation. In the outermost annual rings (between 38 and 44) the strain at maximum stress of latewood decreased and for both types of cells an extensibility of $\approx 1.8\%$ was found. Figure 4(b) shows the maximum strain

from the annual ring of the branch. These values were much higher than those of the stem reaching an extensibility of $\approx 13\%$ for the lower side, where compression wood formation must be part of the explanation.

3.2. Results of the structural investigations

In figure 5(a) a typical scattering pattern of earlywood is shown. For the evaluation of the cellulose MFA, the intensity was integrated over the wave vector of the scattered beam q and plotted versus χ (figure 5(b)). Only one streak of high intensity is visible indicating a very small MFA. The integration yielded a curve that could be fitted with one single Gaussian. The latewood pattern of most annual rings looked

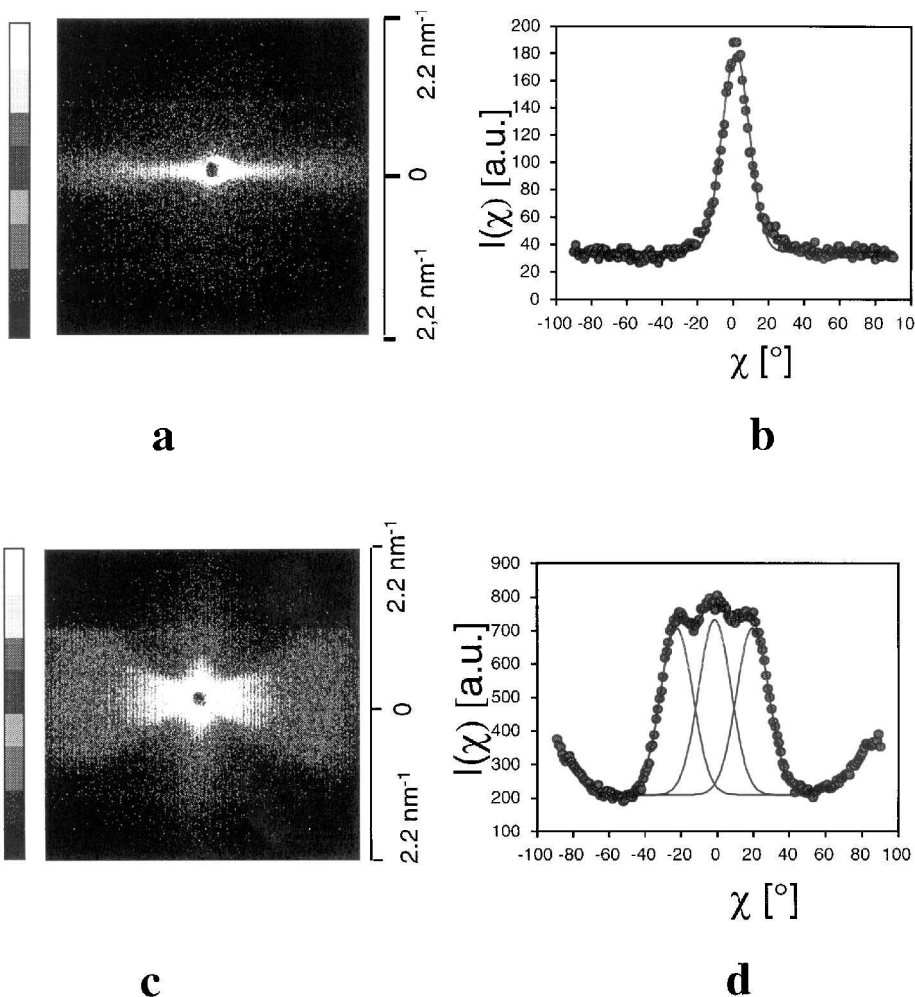


Figure 5. (a) Typical SAXS pattern of earlywood showing only one streak. (b) The intensity was integrated over the wave vector q , plotted versus χ and fitted with one Gaussian. (c) SAXS pattern of latewood of annual rings 17–37 showing three streaks. (d) The intensity was integrated over the wave vector q , plotted versus χ and fitted with three Gaussians.

quite different (figure 5(c)). Three streaks of higher intensity could be distinguished. The integration yielded a curve that could be fitted with three Gaussians (figure 5(d)). For a rectangular cell oriented at right angles to the incoming X-ray beam, the χ values of the inclined streaks directly give the MFA μ ($\chi = \pm\mu$, see equation (3)).

The results for the MFA μ of earlywood and latewood of the 27 annual rings of the stem are shown in figure 6(a). Between the annual rings 17 and 37 the MFA of latewood was found to be $\approx 20^\circ$, whereas the MFA of earlywood was smaller than 5°

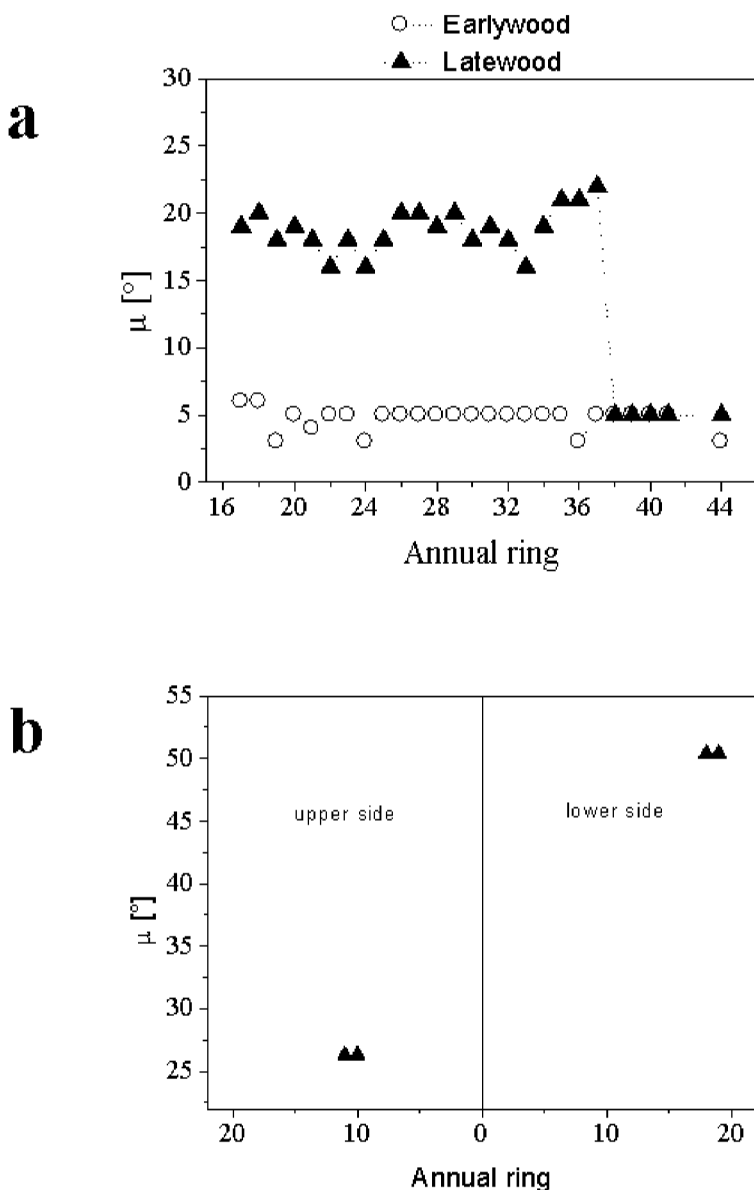


Figure 6. (a) MFA μ versus the investigated annual rings of the stem. After annual ring 37 the MFA of latewood decreased and reached values similar to earlywood. The much higher MFAs of the branch are shown in (b).

indicating an orientation of the cellulose fibrils roughly parallel to the longitudinal direction of the wood cell. Between annual ring 38 and 44, right in the region where the changes in the extensibility of latewood occurred the MFA of latewood dropped dramatically and reached values smaller than 5° similar to earlywood.

Figure 6(b) shows the MFAs of the branch which were higher reaching 26° on the upper and 50° on the lower side.

§ 4. DISCUSSION

The results of the mechanical and structural investigations indicate an interesting relationship between the orientation of the cellulose fibrils in the S2 cell wall layer and the mechanical properties of the wood cell wall. Figure 7 shows the normalized elastic moduli of elasticity versus the MFA. The data points are mean values of all samples from the stem and the branch from annual rings with a MFA $\mu \approx 5^\circ$, $\mu \approx 20^\circ$, $\mu = 26^\circ$ and $\mu = 50^\circ$. The error bars indicate the standard deviation and the numbers show the quantity of samples for each datapoint. The normalized modulus of elasticity decreased in a nonlinear way as the MFAs increased. This behaviour is consistent with earlier results from earlywood of *Pinus radiata* (Cave 1969) and with theoretical predictions (see, for example, Navi *et al.* (1995) and Astley *et al.* (1998)).

The results also suggest a strong correlation between MFA and maximum extensibility (see figure 8). One can clearly see that the MFA in these wood samples, which could be extended by 3.1%, was found to be $\mu \approx 20^\circ$. In contrast, all samples with a MFA in the S2 of smaller than 5° exhibited a maximum strain of only 1.8%, irrespective of whether they consisted of earlywood or latewood cells. The samples of the upper side of the branch with a MFA of 26° could be extended by $\approx 6\%$ and those of the lower side with a very large MFA of 50° exhibited a maximum strain of

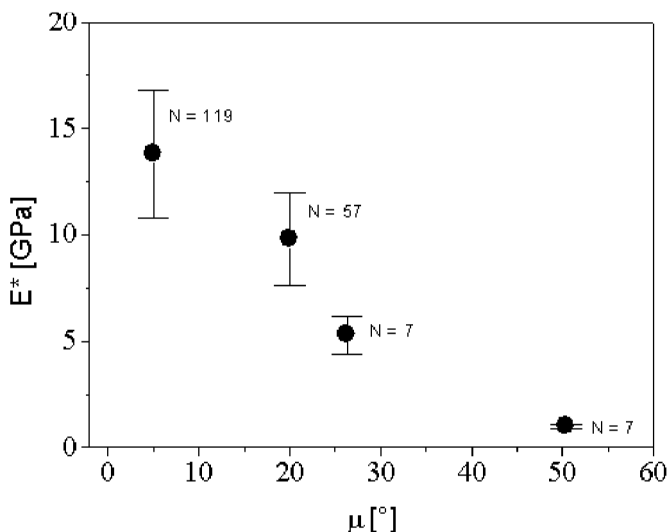


Figure 7. Normalized modulus of elasticity E^* versus the MFA μ . The numbers indicate the quantity of samples for each datapoint. Bars give standard deviation.

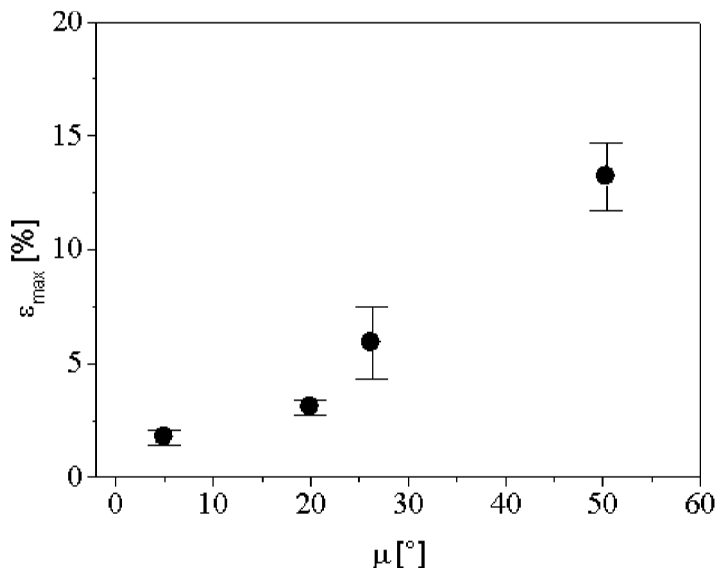


Figure 8. Strain at maximum stress ε_{\max} versus the MFA μ .

$\approx 13\%$. This suggests the conclusion that the MFA μ has a pronounced influence on the extensibility of the cell wall. In figure 9 the stress–strain curves of an earlywood sample with $\mu < 5^\circ$, a latewood sample with $\mu < 5^\circ$, a latewood sample with $\mu = 20^\circ$, a sample of the upper side of the branch with $\mu = 26^\circ$ and a sample of the lower side

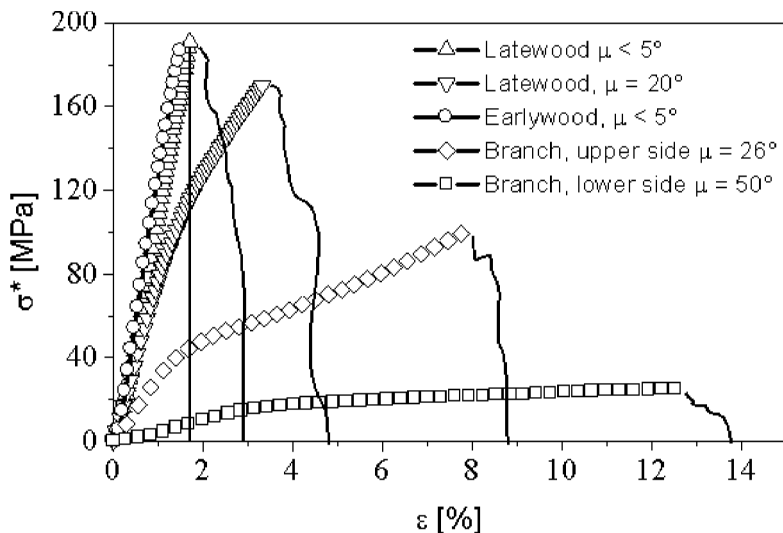


Figure 9. Typical normalized stress–strain curves for earlywood and latewood and wood from the branch. Brittle fracture always occurred in earlywood with cellulose MFAs $< 5^\circ$, while latewood and wood from the branch continued to bear load even beyond the maximum stress point, irrespective of the MFA. The beginning of the curves without symbols indicate the strain at maximum stress ε_{\max} .

with $\mu = 50^\circ$ are depicted. The stress σ was normalized by the ratio ρ_0/ρ to obtain density independent values

$$\sigma^* = \sigma \rho_0 / \rho, \quad (5)$$

characterizing the stress inside the cell wall. It is most interesting that not only the maximum value of the strain but also the whole stress-strain curves of the samples with $\mu < 5^\circ$ were nearly identical until the maximum stress was reached, although one of them consisted of earlywood and the other one of latewood.

After initiation of the macrocrack at maximum stress, the situation changed: earlywood fractured in a brittle way while latewood, regardless of the MFA, always bore load evenly beyond the maximum stress point (compare figure 9). This behaviour was also found for the branch wood. Moreover, one can clearly see that the elastic range is smaller for samples with higher MFAs. The part of the stress-strain curves beyond the elastic range increases with increasing MFA.

We believe that these findings make it obvious that one of the reasons for larger fibrillar angles in the wood cell wall is the optimization of extensibility. Moreover, there is a dramatic increase in extensibility for the samples of the branch, especially for those of the lower side with very large MFAs. This corresponds well with the fact that in a branch much larger strains are to be expected owing to movements in the winds and from gravitational forces. However, one has to take into consideration that other anatomical features like cell wall diameter or cell size vary and that at the bottom of the branch compression wood is formed which is known to have less cellulose and more lignin than normal wood (see, for example, Wardrop and Dadswell (1951) and Core *et al.* (1979)). These parameters might also influence the mechanical properties. Nevertheless our results show a distinct relationship between MFA and extensibility, and MFA and stiffness. The reason why the MFA changes abruptly at the annual ring 38 of the stem remains unknown. Since we have found this effect in the outer annual rings of a number of trees, one may speculate that either environmental effects or the lack of a mechanical stimulus in a stem with a sufficiently large diameter might be responsible for these structural changes.

§ 5. CONCLUSIONS

In this paper tensile tests and small angle X-ray scattering were used to investigate the relationship between mechanical properties and the structure at nanometre level of wood cell walls throughout 27 annual rings of a stem and 2 annual rings of the lower and upper side of a branch of *Picea abies*. The experimental results establish that there is a strong correlation between the MFA of the cellulose fibrils in the S2 cell wall layer and the modulus of elasticity on the one hand, and the strain at maximum stress, characterizing the extensibility of the cell wall, on the other hand. While it has already been found before that small MFAs provide optimum stiffness of the cell wall, this picture now has to be completed: it is obvious that the optimization of the extensibility must be regarded as another important function of the MFA. Thus we may conclude that the variation of fibril angles provides an optimum combination of stiffness (small angles) and extensibility (large angles), in response to the actual mechanical demands in various parts of a tree.

ACKNOWLEDGEMENT

Financial support by the Fonds zur Förderung der Wissenschaftlichen Forschung (Proj. P10729-BIO) is gratefully acknowledged.

REFERENCES

- ASTLEY, R. J., STOL, K. A., and HARRINGTON, J. J., 1998, *Holz als Roh- und Werkstoff*, **56**, 43.
- CAVE, I. D., 1969, *Wood Sci. Technol.*, **3**, 40.
- CAVE, I. D., and WALKER, J. C. F., 1994, *Forest Products J.*, **44**, 43.
- CORE, H. A., CÔTÉ, W. A., and DAY, A. C., 1979, *Wood Structure and Identification* (Syracuse, NY: Syracuse University Press).
- DINWOODIE, J. M., 1989, *Nature's Cellular Polymeric Fibre-composite* (London: The Institute of Metals).
- FEIGIN, L. A., and SVERGUN, D. I., 1978, *Structure Analysis by Small-Angle X-ray and Neutron Scattering* (New York: Plenum Press).
- FENGEL, D., and WEGENER, G., 1989, *Wood—Chemistry, Ultrastructure, Reactions* (Berlin, New York: De Gruyter).
- GLATTER, O., and KRATKY, O. (eds), 1982, *Small-Angle X-ray Scattering* (London: Academic Press).
- GUINIER, A., and FOURNET, G., 1955, *Small-Angle Scattering of X-rays* (New York: Wiley).
- JAKOB, H. F., FENGEL, D., TSCHIEGG, S. E., and FRATZL, P., 1995, *Macromolecules*, **26**, 8782.
- JAKOB, H. F., TSCHIEGG, S. E., and FRATZL, P., 1994, *J. Struct. Biol.*, **113**, 13.
- LICHTENEGGER, H., REITERER, A., TSCHIEGG, S., and FRATZL, P., 1998, *Microfibril Angle in Wood, Proceedings of the International Association of Wood Anatomists*, West Port, New Zealand, edited by B. Butterfield, p. 140.
- MARK, R. E., 1967, *Cell Wall Mechanics of Tracheids* (New Haven, London: Yale University Press).
- MEYLAN, B. A., 1972, *Wood Sci. Technol.*, **6**, 293.
- NAVI, P., RASTOGI, P. K., GRESSE, V., and TÖLOU, A., 1995, *Wood Sci. Technol.*, **29**, 411.
- PAGE, D. H., and EL-HOSSEINY, F., 1983, *J. Pulp Paper Sci.*, **9**, 1.
- PAGE, D. H., EL-HOSSEINY, F., and WINKLER, K., 1971, *Nature*, **229**, 252.
- PERRET, R., and RULAND, W., 1969, *J. appl. Cryst.*, **2**, 209.
- PRESTON, R. D., 1946, *Proc. Roy. Soc. B*, **133**, 327.
- REITERER, A., JAKOB, H. F., STANZL-TSCHIEGG, S. E., and FRATZL, P., 1998, *Wood Sci. Technol.*, **32**, 335.
- WARDROP, A. B., and DADSWELL, H. E., 1951, *Austral. J. Sci. Res. B*, **4**(4), 391.